

**The following resources related to this article are available online at [www.sciencemag.org](http://www.sciencemag.org) (this information is current as of September 22, 2009 ):**

**Updated information and services**, including high-resolution figures, can be found in the online version of this article at:

<http://www.sciencemag.org/cgi/content/full/325/5942/874>

**Supporting Online Material** can be found at:

<http://www.sciencemag.org/cgi/content/full/325/5942/874/DC1>

This article **cites 31 articles**, 14 of which can be accessed for free:

<http://www.sciencemag.org/cgi/content/full/325/5942/874#otherarticles>

This article appears in the following **subject collections**:

Cell Biology

[http://www.sciencemag.org/cgi/collection/cell\\_biol](http://www.sciencemag.org/cgi/collection/cell_biol)

Information about obtaining **reprints** of this article or about obtaining **permission to reproduce this article** in whole or in part can be found at:

<http://www.sciencemag.org/about/permissions.dtl>

# Mechanistic Analysis of a Dynamin Effector

Laura L. Lackner, Jennifer S. Horner, Jodi Nunnari\*

Dynamin-related proteins (DRPs) can generate forces to remodel membranes. In cells, DRPs require additional proteins [DRP-associated proteins (DAPs)] to conduct their functions. To dissect the mechanistic role of a DAP, we used the yeast mitochondrial division machine as a model, which requires the DRP Dnm1, and two other proteins, Mdv1 and Fis1. Mdv1 played a postmitochondrial targeting role in division by specifically interacting and coassembling with the guanosine triphosphate-bound form of Dnm1. This regulated interaction nucleated and promoted the self-assembly of Dnm1 into helical structures, which drive membrane scission. The nucleation of DRP assembly probably represents a general regulatory strategy for this family of filament-forming proteins, similar to F-actin regulation.

**D**ynamin-related proteins (DRPs) comprise a family of large guanosine triphosphatases (GTPases) that self-assemble into structures that associate with and remodel intracellular membranes (1–3). In vitro, DRPs are sufficient to mediate membrane constriction and scission (4–8). In vivo, however, DRP-associated proteins (DAPs) are required for DRP-dependent membrane remodeling (1, 9–15). Although many DAPs have been identified, their mechanistic roles are unknown. We examined the role of Mdv1, a DAP required for mitochondrial division, which is driven by the action of the DRP Dnm1 (3). Guanosine triphosphate (GTP) drives the self-assembly of Dnm1 into helical structures, which can constrict lipid membranes (5). Self-assembly stimulates Dnm1 GTP hydrolysis, which is required to complete mitochondrial scission (5, 16). Dnm1 self-assembly proceeds via a rate-limiting, Dnm1 concentration-dependent nucleation event, which may be exploited as a means to regulate the assembly and thus the function of Dnm1 in vivo (5).

Department of Molecular and Cellular Biology, University of California, Davis, CA 95616, USA.

\*To whom correspondence should be addressed. E-mail: jnunnari@ucdavis.edu

Dnm1-driven mitochondrial division also requires Fis1 and Mdv1 (10, 17–19). Mdv1 functions as a molecular bridge between mitochondrial-anchored Fis1 and soluble Dnm1, and together Fis1 and Mdv1 function to target Dnm1 to the mitochondrial surface (10, 20–22). Mdv1 also functions after targeting to facilitate division (16, 20) [supporting online material (SOM) text and fig. S1]. To examine the post-targeting roles of Mdv1, we purified it from yeast cells. Co-overexpression of Fis1 lacking the transmembrane domain Fis1 $\Delta$ TM was required to produce a soluble form of full-length Mdv1, and Fis1 $\Delta$ TM co-purified with Mdv1 at stoichiometric levels (fig. S2A). However, after purification, the Mdv1/Fis1 $\Delta$ TM complex dissociated (fig. S2B).

We asked whether the interaction of Mdv1 and/or Fis1 with Dnm1 was regulated and whether they affected Dnm1's kinetic and structural properties. Using a nonphysiological liposome composition, we targeted Dnm1 directly to liposomes. Dnm1 bound efficiently to liposomes in a manner that was independent of guanine nucleotides (Fig. 1A). Consistently, the Dnm1 mutants Dnm1S42N and Dnm1K41A, which are deficient in nucleotide binding or nucleotide hydrolysis, respectively, also efficiently bound to liposomes (5, 16). Only the assembly-defective mutant Dnm1G385D, which

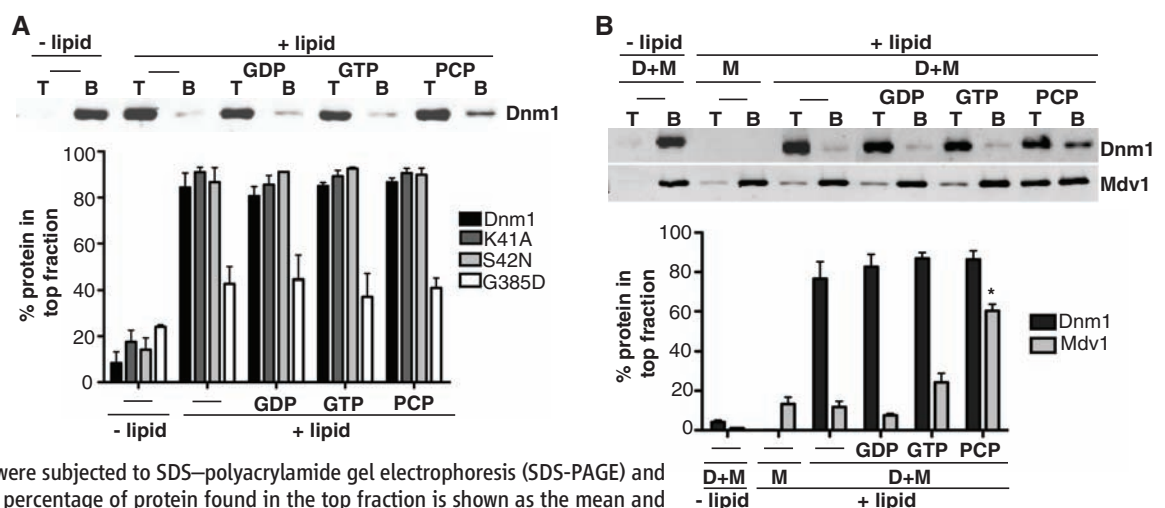
exists as a dimer under assay conditions, exhibited a decreased association with liposomes (5, 23). Thus, unassembled Dnm1 has a relatively weak affinity for liposomes, and the interaction between oligomeric Dnm1 and liposomes is strengthened via avidity.

In contrast to Dnm1, the recruitment of Mdv1 to liposomes required Dnm1 and either GTP or the nonhydrolyzable GTP analog GMPPCP (Fig. 1B). In contrast to Mdv1, only a small fraction (10 to 20%) of Fis1 $\Delta$ TM was recruited to Dnm1-liposome complexes, and the addition of a 10-fold molar excess of Fis1 $\Delta$ TM did not alter the amount of Dnm1 associated with liposomes nor the amount of Mdv1 recruited to Dnm1-liposome complexes (fig. S2C). Thus, Fis1 had no measurable effect on the Dnm1-lipid or Dnm1-Mdv1 interaction.

Consistent with a GTP-regulated Dnm1-Mdv1 interaction, Dnm1K41A also was able to efficiently recruit Mdv1 to liposomes in the presence of both GTP and GMPPCP, whereas Dnm1S42N was not able to recruit Mdv1 to liposomes (fig. S3A and B). The increased recruitment of Mdv1 to liposomes by Dnm1K41A with GTP as compared to wild-type Dnm1 suggests that upon nucleotide hydrolysis, the Dnm1-Mdv1 interaction was destabilized (Fig. 1B and fig. S3A). Assembly-defective Dnm1G385D was not able to efficiently recruit Mdv1 to liposomes in the presence of GTP or GMPPCP, a finding that is consistent with previous studies (fig. S3C) (16).

Thus, the Dnm1-Mdv1 interaction is dependent on a combination of avidity and the GTP-specific conformational state of Dnm1. Liposomes facilitated the assembly of Dnm1 helical structures in a nucleotide-independent manner, in contrast to the strict GTP requirement for the assembly of Dnm1 helices in the absence of liposomes (fig. S4A) (5). Thus, although avidity is probably important, the GTP-specific conformational state of Dnm1 is the critical determinant for the Dnm1-Mdv1 interaction. Indeed, qualitative differences in the helical structures formed in the presence of GMPPCP were observed (fig. S4A). Thus, Mdv1

**Fig. 1.** Mdv1 preferentially interacts with the GTP-bound form of Dnm1. (A) Dnm1 and the indicated Dnm1 mutants at 0.4  $\mu$ M were incubated with liposomes in the absence and presence of various nucleotides. The association of the protein with liposomes was assessed by its ability to float with liposomes after equilibrium sucrose gradient centrifugation. Equivalent amounts of the top (T) and bottom (B)



fractions of the gradients were subjected to SDS-polyacrylamide gel electrophoresis (SDS-PAGE) and Western blot analysis. The percentage of protein found in the top fraction is shown as the mean and SEM;  $n = 3$  independent experiments. (B) Dnm1 and Mdv1, each at 0.4  $\mu$ M, were incubated with liposomes in the absence and presence of various nucleotides and subjected to liposome floatation and analysis as described in (A). Data are shown as the mean and SEM;  $n = 3$  independent experiments. \* $P \leq 0.05$ .

preferentially interacts with the GTP-bound, assembled form of Dnm1, and this interaction is regulated by GTP hydrolysis, which probably reflects the importance of a dynamic Dnm1-Mdv1 interaction in division *in vivo* (16).

A GTP-regulated Dnm1-Mdv1 interaction is consistent with a role for Mdv1 in regulating Dnm1 self-assembly and activity. To test this idea, we examined whether purified Mdv1 altered the kinetic properties of Dnm1 (5). As previously observed, Dnm1 exhibited a concentration-dependent kinetic lag in assembly-driven GTP hydrolysis before reaching a steady state, indicating that a nucleation event is required for self-assembly (5) (Fig. 2, A and B). The addition of Mdv1 dramatically decreased this kinetic lag in a concentration-dependent manner (Fig. 2, A and B). Thus, Mdv1 acts as a nucleator for Dnm1 self-assembly. The nucleation of Dnm1 self-assembly was also stimulated by liposomes with a mitochondrial outer membrane composition (OMC) (Fig. 2A) (24). Under the conditions tested, OMC liposomes were less effective than Mdv1 in decreasing the kinetic

lag and, in combination with Mdv1, did not further reduce the kinetic lag.

Mdv1 also increased the steady-state level of GTP hydrolysis by Dnm1, which also indicates that Mdv1 stimulated Dnm1 self-assembly (Fig. 2, C and D). The addition of Mdv1 also reduced the apparent Hill coefficient for GTP binding (Fig. 2D), which suggests that Mdv1 is inducing and/or stabilizing a GTP-dependent conformation of Dnm1 to promote self-assembly. The addition of Mdv1 resulted in a  $1.4 \pm 0.1$ -fold increase ( $n = 3$  independent experiments) in the amount of GTP that could be cross-linked to Dnm1 by ultraviolet light (fig. S5), consistent with Mdv1 increasing the affinity of Dnm1 for GTP and preferentially binding to the GTP-bound form of Dnm1 (Fig. 1B). No significant effect on Dnm1 activity with or without Mdv1 was observed with a 15-fold molar excess of Fis1 $\Delta$ TM, suggesting that Fis1 does not act directly on Dnm1 during mitochondrial division (fig. S2, D and E).

Mdv1 modulated Dnm1 activity only within the range of Dnm1 concentrations observed *in vivo*

(Fig. 2E and table S1). OMC liposomes also had the greatest stimulatory effect on Dnm1 activity within this range, albeit to a lesser extent than Mdv1 (Fig. 2E). When added in combination with Mdv1, OMC liposomes did not further stimulate the activity of Dnm1. At relatively high nonphysiological concentrations, Dnm1 was able to effectively nucleate its own self-assembly, and the addition of Mdv1 and OMC liposomes had no further effect on the rate of GTP hydrolysis. Thus, because maximal GTP hydrolysis by Dnm1 is unaltered by Mdv1, Mdv1 does not stimulate the intrinsic ability of Dnm1 to hydrolyze GTP and thus acts as a positive effector to nucleate and drive Dnm1 assembly at the mitochondrial outer membrane, and consequently the GTP hydrolysis activity of Dnm1 is stimulated.

Kinetic data indicate that Mdv1 acts as a nucleator to drive Dnm1 self-assembly. Velocity sedimentation analysis consistently revealed that a greater fraction of Dnm1 was recovered in the assembled pellet fraction in the presence of Mdv1 and either GTP or GMPPCP, as compared to that recovered under identical assay conditions with Dnm1 alone (Fig. 3A). Moreover, a greater fraction of Mdv1 was recovered in the pellet in the presence of Dnm1 and either GTP or GMPPCP. Thus, Mdv1 acts to facilitate Dnm1 assembly by preferentially interacting with the GTP-bound form of Dnm1 and nucleating its assembly. In agreement with this idea, Mdv1 counteracts the effects of the Dnm1 small-molecule inhibitor mdv1-1, which attenuates the GTP-dependent assembly of Dnm1 (25) (SOM text and fig. S6).

To determine the structural basis for Mdv1-dependent Dnm1 nucleation, we analyzed GMPPCP Dnm1 structures by negative-stain electron microscopy (EM) (Fig. 3, B and C). At physiological Dnm1 concentrations, in the absence of Mdv1, we observed both simple rings and helices (Fig. 3B). In contrast, in the presence of Mdv1, we exclusively observed helices (Fig. 3B), which were uniformly decorated with additional electron density (Fig. 3, B and C). Consistently, Dnm1 structures assembled in the presence of liposomes and Mdv1 displayed an increase in electron density, quantified as an increase in the distance from the lipid membrane to the outer edge of the assembled protein, as well as a qualitative difference in structural features (Fig. 3, D and E). Thus, Mdv1 coassembled with Dnm1 helical structures, probably at a stoichiometric ratio as suggested by our binding data (Fig. 1B and fig. S3).

Based on our analyses, we propose two models for Mdv1-dependent Dnm1 nucleation, which are not mutually exclusive (fig. S7). Our finding that Mdv1 binds preferentially to Dnm1-GTP supports a model in which it acts as a conformational nucleator to induce or stabilize a GTP-like conformation of Dnm1 that is more favorable for self-assembly. Alternatively, Mdv1 may function as a structural nucleator by acting as a physical scaffold to facilitate the formation or stabilization of oligomeric Dnm1 assemblies. To test this possibility, we examined whether Mdv1 itself could oligomerize. In yeast two-hybrid studies, the central coiled-coil domain of Mdv1 can mediate self-interaction (20). Examina-

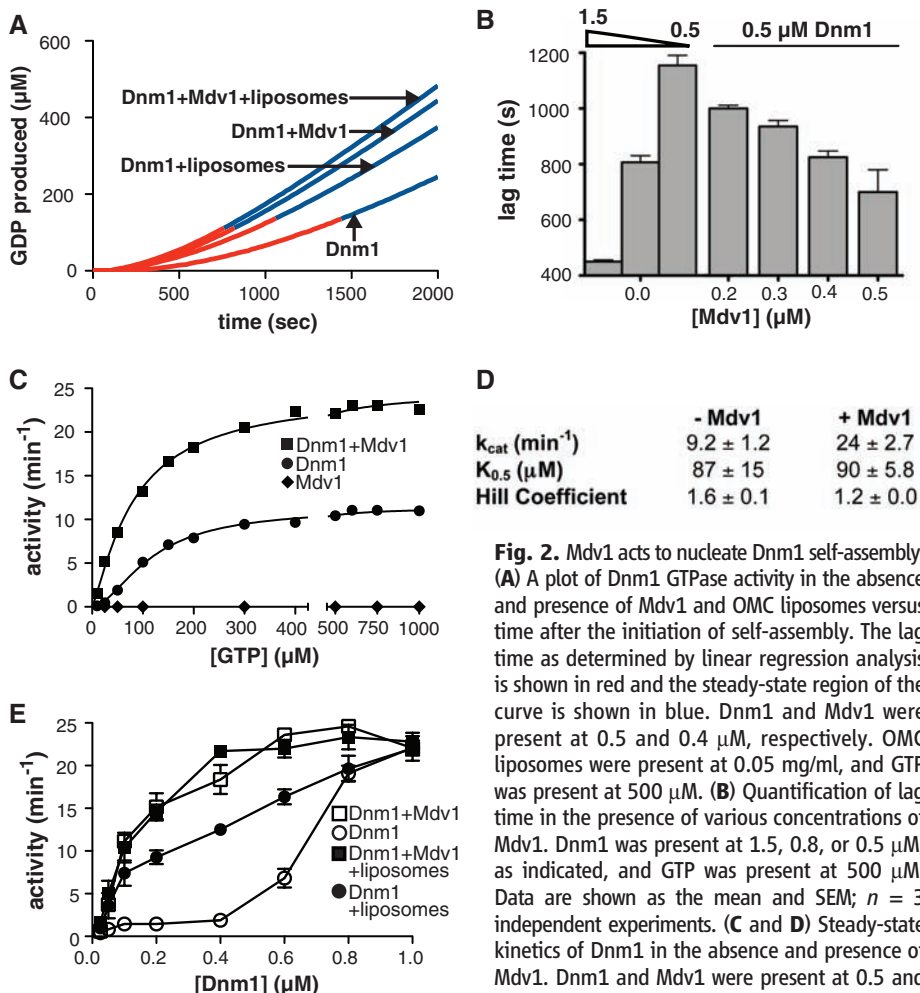


**Fig. 2.** Mdv1 acts to nucleate Dnm1 self-assembly. (A) A plot of Dnm1 GTPase activity in the absence and presence of Mdv1 and OMC liposomes versus time after the initiation of self-assembly. The lag time as determined by linear regression analysis is shown in red and the steady-state region of the curve is shown in blue. Dnm1 and Mdv1 were present at 0.5 and 0.4  $\mu\text{M}$ , respectively. OMC liposomes were present at 0.05 mg/ml, and GTP was present at 500  $\mu\text{M}$ . (B) Quantification of lag time in the presence of various concentrations of Mdv1. Dnm1 was present at 1.5, 0.8, or 0.5  $\mu\text{M}$ , as indicated, and GTP was present at 500  $\mu\text{M}$ . Data are shown as the mean and SEM;  $n = 3$  independent experiments. (C and D) Steady-state kinetics of Dnm1 in the absence and presence of Mdv1. Dnm1 and Mdv1 were present at 0.5 and 0.4  $\mu\text{M}$ , respectively. A representative kinetic

experiment is shown in (C). The table in (D) shows kinetic parameters determined as described in methods (32).  $k_{\text{cat}}$ , turnover number;  $K_{0.5}$ , substrate concentration where velocity is one-half maximal. Data are shown as the mean and SEM;  $n = 3$  independent experiments. (E) Steady-state GTP hydrolysis activity of Dnm1 at various Dnm1 concentrations in the absence and presence of 0.4  $\mu\text{M}$  Mdv1 and 0.05 mg/ml OMC liposomes, as indicated. GTP was present at 500  $\mu\text{M}$ . Data are shown as the mean and SEM;  $n = 3$  independent experiments.

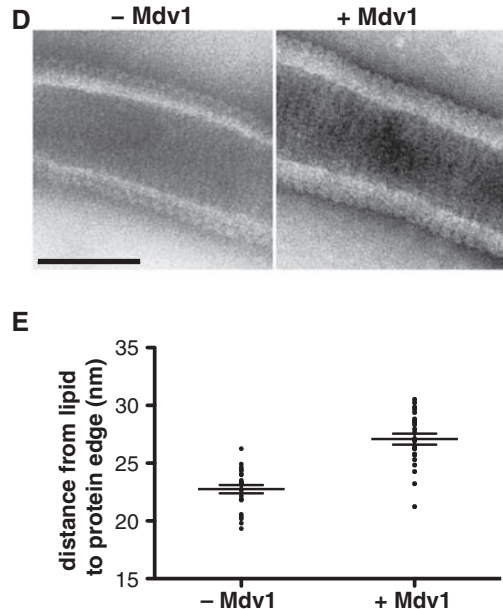
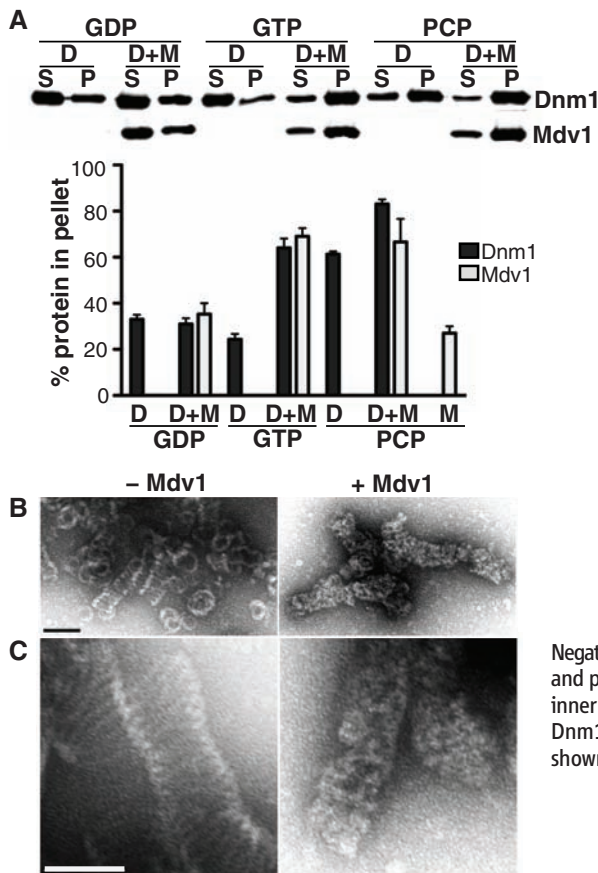


**Fig. 3.** Mdv1 stimulates Dnm1 self-assembly. (A) Velocity sedimentation of Dnm1 in the absence and presence of Mdv1. Dnm1 and Mdv1 were present at 0.2  $\mu$ M. A representative Western blot is shown, and quantification data are shown as the mean and SEM;  $n = 3$  independent experiments. (B and C) Analysis of GMPPCP-dependent Dnm1 self-assembly by negative-stain EM in the absence (left panels) and presence (right panels) of Mdv1. Different fields are shown in (B) and (C); the images in (C) were taken at a magnification 15,000 times higher than those in (B). Scale bars, 100 nm. (D) Negative-stain EM images of Dnm1-GMPPCP assembled on liposomes in the absence (left panel) and presence (right panel) of Mdv1. Scale bar, 100 nm. (E) Quantification of the distance from the inner edge of the lipid membrane to the outer edge of the assembled protein on Dnm1- and Dnm1-Mdv1 coated liposomes;  $n = 24$  protein-coated liposomes. The mean and SEM are also shown.

tion of the subunit composition of purified Mdv1 by hydrodynamic analysis indicated that it exists as a dimer (Fig. 4A). At higher concentrations, we also detected Mdv1 tetramers and hexamers after treatment with a chemical cross-linker (Fig. 4B). Thus, like Dnm1, dimeric Mdv1 is probably the building block for larger Mdv1 oligomers, which is consistent with Dnm1 and Mdv1 acting in a stoichiometric manner (5). In addition, these results support the idea that through self-assembly, Mdv1 can also act as a structural nucleator for Dnm1 self-assembly.

It is likely that the nucleation of DRP assembly will emerge as a general strategy for the regulation of DRP function in vivo by DAPs. Indeed, the assembly of dynamin can be promoted by DAPs, such as amphiphysin and Snx9 (9, 13–15). Mdv1 is tethered to the mitochondrial surface by Fis1 (10). Thus, Mdv1-dependent nucleation serves to spatially activate Dnm1's membrane remodeling function within the cell. The temporal and contextual regulation of DRPs by DAPs is probably also important. This is apparent in mammalian cells, where the mammalian Dnm1 ortholog, Drp1, is less assembled than Dnm1 at a steady state, and mitochondrial division is stimulated by a variety of signaling pathways, which serve to integrate mitochondrial division with cellular physiology or to perform other functions, such as the regulation of mitochondrial outer membrane permeabilization during apoptosis (25–28). Although no Mdv1 ortholog has been identified in mammalian cells, multiple DAP candidates have been identified for Drp1, raising

**Fig. 4.** Mdv1 oligomerizes. (A) Hydrodynamic parameters of Mdv1 were determined by sucrose gradient and gel filtration analyses and calculated as described in methods (32). (B) Analysis of Mdv1 oligomerization by chemical cross-linking. SDS-PAGE Coomassie-stained gel is shown of Mdv1 samples without (lane 1) and with (lane 2) a 5-M excess of cross-link reagent.

the possibility that each may function as an effector that responds to a different cellular input (29–31). Finally, it is also possible that mechanistically distinct DAPs exist that serve as partial, negative, or neutral effectors. Thus, DAPs might also function in cells to expand the repertoire of DRP functions.

**References and Notes**

1. J. E. Hinshaw, *Annu. Rev. Cell Dev. Biol.* **16**, 483 (2000).
2. G. J. Praefcke, H. T. McMahon, *Nat. Rev. Mol. Cell Biol.* **5**, 133 (2004).
3. S. Hoppins, L. Lackner, J. Nunnari, *Annu. Rev. Biochem.* **76**, 751 (2007).
4. J. E. Hinshaw, S. L. Schmid, *Nature* **374**, 190 (1995).
5. E. Ingerman *et al.*, *J. Cell Biol.* **170**, 1021 (2005).
6. A. Roux, K. Uyhazi, A. Frost, P. De Camilli, *Nature* **441**, 528 (2006).
7. P. V. Bashkirov *et al.*, *Cell* **135**, 1276 (2008).
8. T. J. Pucadyil, S. L. Schmid, *Cell* **135**, 1263 (2008).
9. K. Takei, V. I. Slepnev, V. Haucke, P. De Camilli, *Nat. Cell Biol.* **1**, 33 (1999).
10. Q. Tieu, J. Nunnari, *J. Cell Biol.* **151**, 353 (2000).

11. K. L. Cerveny, S. L. Studer, R. E. Jensen, H. Sesaki, *Dev. Cell* **12**, 363 (2007).
12. K. Farsad *et al.*, *J. Cell Biol.* **155**, 193 (2001).
13. F. Soulet, D. Yazar, M. Leonard, S. L. Schmid, *Mol. Biol. Cell* **16**, 2058 (2005).
14. Y. Yoshida *et al.*, *EMBO J.* **23**, 3483 (2004).
15. R. Ramachandran, S. L. Schmid, *EMBO J.* **27**, 27 (2008).
16. K. Naylor *et al.*, *J. Biol. Chem.* **281**, 2177 (2006).
17. A. D. Mozdy, J. M. McCaffery, J. M. Shaw, *J. Cell Biol.* **151**, 367 (2000).
18. P. Fekkes, K. A. Shepard, M. P. Yaffe, *J. Cell Biol.* **151**, 333 (2000).
19. K. L. Cerveny, J. M. McCaffery, R. E. Jensen, *Mol. Biol. Cell* **12**, 309 (2001).
20. Q. Tieu, V. Okreglak, K. Naylor, J. Nunnari, *J. Cell Biol.* **158**, 445 (2002).
21. M. A. Karren, E. M. Coonrod, T. K. Anderson, J. M. Shaw, *J. Cell Biol.* **171**, 291 (2005).
22. E. E. Griffin, J. Graumann, D. C. Chan, *J. Cell Biol.* **170**, 237 (2005).
23. R. E. Jensen, A. E. Hobbs, K. L. Cerveny, H. Sesaki, *Microsc. Res. Tech.* **51**, 573 (2000).
24. G. Daum, *Biochim. Biophys. Acta* **822**, 1 (1985).
25. A. Cassidy-Stone *et al.*, *Dev. Cell* **14**, 193 (2008).

26. R. J. Youle, *Dev. Cell* **8**, 298 (2005).  
 27. L. L. Lackner, J. M. Nunnari, *Biochim. Biophys. Acta*, 10.1016/j.bbdis.2008.11.011 (2008).  
 28. J. Bereiter-Hahn, M. Voth, *Microsc. Res. Tech.* **27**, 198 (1994).  
 29. Y. Yoon, E. W. Krueger, B. J. Oswald, M. A. McNiven, *Mol. Cell. Biol.* **23**, 5409 (2003).  
 30. M. Karbowski, S. Y. Jeong, R. J. Youle, *J. Cell Biol.* **166**, 1027 (2004).  
 31. S. Gandre-Babbe, A. M. van der Blik, *Mol. Biol. Cell* **19**, 2402 (2008).  
 32. Materials and methods are available as supporting material on Science Online.  
 33. We thank J. Evans for technical EM advice and help with analysis of Dnm1-Mdv1 structures; G. Adamson, J. Hinshaw, J. Mears, and H. Stahlberg for technical EM advice; A. Cassidy-Stone for providing the mdvi-1 data; and members of the Nunnari lab for critical discussions and comments. J.N. is supported by NIH grant R01GM062942. L.L.L. is supported by NIH postdoctoral fellowship 1F32GM078749.

## Supporting Online Material

www.sciencemag.org/cgi/content/full/325/5942/874/DC1  
 Materials and Methods  
 SOM Text  
 Figs. S1 to S7  
 Table S1  
 References

27 May 2009; accepted 29 June 2009  
 10.1126/science.1176921

# ER Stress Controls Iron Metabolism Through Induction of Hepcidin

Chiara Vecchi,<sup>1</sup> Giuliana Montosi,<sup>1</sup> Kezhong Zhang,<sup>2</sup> Igor Lamberti,<sup>1</sup> Stephen A. Duncan,<sup>3</sup> Randal J. Kaufman,<sup>4</sup> Antonello Pietrangelo<sup>1\*</sup>

Hepcidin is a peptide hormone that is secreted by the liver and controls body iron homeostasis. Hepcidin overproduction causes anemia of inflammation, whereas its deficiency leads to hemochromatosis. Inflammation and iron are known extracellular stimuli for hepcidin expression. We found that endoplasmic reticulum (ER) stress also induces hepcidin expression and causes hypoferrremia and spleen iron sequestration in mice. CREBH (cyclic AMP response element-binding protein H), an ER stress-activated transcription factor, binds to and transactivates the hepcidin promoter. Hepcidin induction in response to exogenously administered toxins or accumulation of unfolded protein in the ER is defective in CREBH knockout mice, indicating a role for CREBH in ER stress-regulated hepcidin expression. The regulation of hepcidin by ER stress links the intracellular response involved in protein quality control to innate immunity and iron homeostasis.

The iron-regulatory hormone hepcidin, a defensin-like peptide produced by the hepatocytes in response to iron and inflammation, is a central humoral mediator of innate immunity and host defense (1). The primary antimicrobial strategy of this circulating peptide may be that of limiting vital iron that is needed by invading microorganisms, thus contributing to host defense. Hepcidin accomplishes this task by triggering degradation of the iron exporter ferroportin, thereby limiting iron egress from enterocytes and macrophages (2). If perpetuated, hepcidin stimulation may lead to the anemia of chronic diseases that is seen during infection, malignancy, and chronic inflammation (3). Thus, hepcidin qualifies as an acute-phase protein and an important component of the innate immune response.

Recently, the acute inflammatory response has been linked to endoplasmic reticulum (ER) stress, a state that is associated with disruption of ER homeostasis and accumulation of unfolded or misfolded proteins in the ER. CREBH, an ER stress-associated liver-specific transcription factor, responds to the immune response-inducing factors lipopolysaccharide (LPS) and interleukin-6 (IL-6) and directly

activates the transcription of acute-phase response genes, such as serum amyloid P component (SAP) and C-reactive protein (CRP) in the liver (4). Both

LPS and IL-6 are also potent inducers of hepcidin in the liver (5, 6). Based on these premises, we wondered whether hepcidin, the iron hormone, is controlled by ER stress and investigated the contribution of CREBH to this activity.

We first tested three known ER stressors in the HepG2 hepatoma cell line: brefeldin A, the A23187 ionophore, and tunicamycin (Tm) (7). As expected, all tested compounds induced ER stress, as shown by the appearance of the spliced form of XBP1, an indicator of ER stress (8) (Fig. 1). Under such circumstances, the expression of hepcidin mRNA was markedly induced, particularly by Tm and A23187 (Fig. 1, A to C). Actinomycin D completely prevented Tm-induced hepcidin mRNA stimulation, indicating that hepcidin response to ER stress is due to transcriptional activation (Fig. 1D).

To confirm the in vitro data, we performed further experiments in mice treated with Tm and found that ER stress readily induces hepatic hepcidin gene expression in vivo (Fig. 2A). In agreement with the hepcidin model of iron regulation, Tm-treated mice

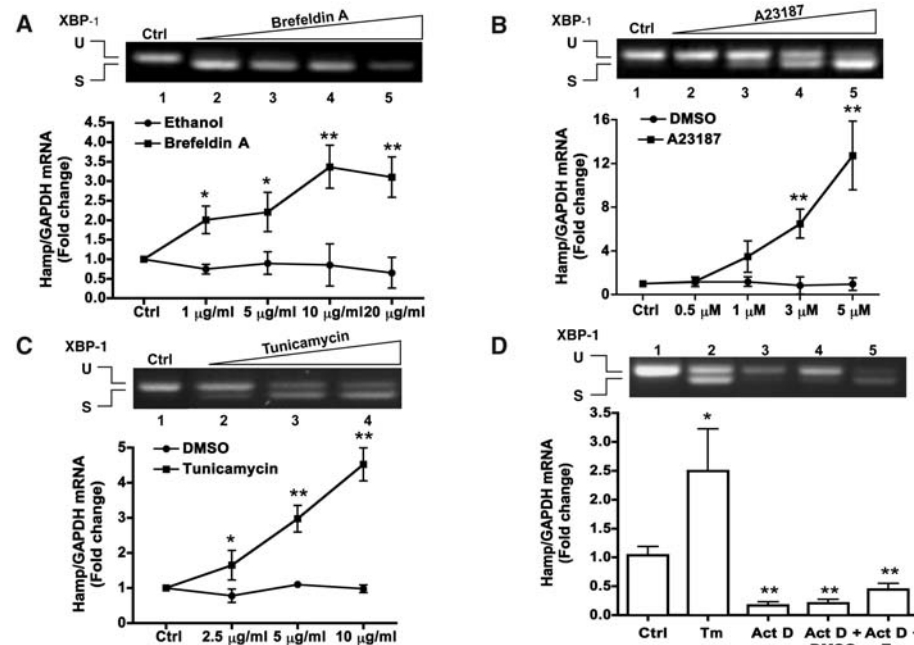


**Fig. 1.** ER stress induces hepcidin gene expression in vitro. (A to C) HepG2 cells were treated with different ER stressors, as indicated. RNA was extracted and subjected to semiquantitative reverse transcription-polymerase chain reaction (RT-PCR) for unspliced (U, 442 bp) or spliced (S, 416 bp) XBP1 mRNA forms (shown in the upper panel by ethidium bromide stain) or to quantitative RT-PCR (qRT-PCR) for hepcidin mRNA (HAMP) (shown in the lower graph). Data are the mean  $\pm$  SD of three independent triplicate experiments with mean control values set to 1.0 (\* $P$  < 0.01; \*\* $P$  < 0.001). (D) HepG2 cells were cultured in the absence or presence of actinomycin D (Act D, 1  $\mu$ g/ml) and tunicamycin (Tm, 10  $\mu$ g/ml). RNA was extracted and processed as above. Data are presented and analyzed as above (\* $P$  < 0.03; \*\* $P$  < 0.005).

<sup>1</sup>Center for Hemochromatosis, Department of Internal Medicine, University Hospital Policlinico di Modena, Modena, Italy. <sup>2</sup>Center for Molecular Medicine and Genetics, Wayne State University School of Medicine, Detroit, MI 48201, USA. <sup>3</sup>Department of Cell Biology, Neurobiology, and Anatomy, Medical College of Wisconsin, Milwaukee, WI 53226, USA. <sup>4</sup>Howard Hughes Medical Institute, Departments of Biological Chemistry and Internal Medicine, University of Michigan Medical Center, Ann Arbor, MI 48109-0650, USA.

\*To whom correspondence should be addressed. E-mail: antonello.pietrangelo@unimore.it